Laser direct writing of nanoreliefs in Sn nanofilms

Chuan Fei Guo,[1,2] Zhuwei Zhang,[1,2] Sihai Cao,[1,2] and Qian Liu[1,*]

[1]*National Center for Nanoscience and Technology, No. 11 Beiyitiao, Zhongguancun, Beijing 100190, China*
[2]*Graduate University of the Chinese Academy of Sciences, Beijing 100080, China*
**Corresponding author: liuq@nanoctr.cn*

Received May 15, 2009; revised August 5, 2009; accepted August 14, 2009;
posted August 21, 2009 (Doc. ID 111413); published September 10, 2009

High-resolution (~200 nm) nanoreliefs, which possess a controllable height change (Δh, up to film thickness) and transmittance or reflectance, have been successfully fabricated in 12-nm-thick Sn films by using 532 nm pulsed laser direct writing. Different from current micro/nanofabrication techniques, the height change of the nanoreliefs is generated by a laser-induced-thickening process. The majority of the height change comes from a balling and coarsening effect rather than oxidation of grains. Because both optical density and Δh of the nanoreliefs are almost linear to laser power, the optical images can highly resemble the topographic images. This technique is useful for fabricating complicated nanorelief structures and fine images.

OCIS codes: 220.4241, 310.6628, 090.6186.

With the rapid development of micro/nanofabrication technologies, the micro/nanoreliefs are extremely desirable because they have many potential applications in micro artworks, image storage, anti counterfeiting, micro/nano diffractive optical elements (DOEs), and micro/nano-electro-mechanical-system devices. Although photolithography, e-beam lithography (EBL), nanoimprint lithography (NIL), and focused ion beam (FIB) milling are mainstream technologies to make micro/nanostructure [1–4], they are either too costly or too complicated for fabricating high-resolution relief structures. Dip-pen nanolithography (DPN) is a simpler method to tailor the chemical composition and structure of a surface on nanoscale [5], but it relies on the "ink" and lacks capability for three-dimensional (3D) fabrication. At present, the microreliefs are usually fabricated by using grayscale photolithography [6–8], but it is hard to achieve a sub-500 nm resolution because of limited resolution of the photolithography machine. A lot of efforts in near field optics, two-photon absorption (TPA), and negative refractive index material technique have concentrated on overcoming the diffraction limit [9–11]. Among them, TPA is attractive for making complicated sub-200 nm 3D structures, such as microbulls, photonic crystals, and DOEs [11–13]; however, only transparent polymers can be used as work media, and posttreatments are needed. Laser direct writing (LDW) is a raster-scan technique and has the advantage of not needing templates, masks, or vacuum. LDW has been applied to make micro/nanostructures in many types of materials, including metals, creating simple submicrometer line structures on a metallic film [14]. However, it is still unavailable so far for fabricating complicated high-resolution relief structures in metallic and inorganic materials. In this Letter, complicated high-resolution nanoreliefs were successfully fabricated in metallic Sn films by using LDW, which is maskless and templateless, free of vacuum, and without any posttreatments and pattern transfer. Simultaneously, continuous-tone transmittance and reflectance were found, so that both fine transmitted and reflected images could be obtained.

Sn films with a thickness of 12 nm and a roughness (Rq) of 2 nm were sputtered on glass substrates. A Nd:YAG 532 nm laser was used as beam source of a home-built laser direct writer; the sample was placed on the focal plane of the objective lens (NA 0.95, Nikon) for the raster scanning with a power ranging from 0 to 8 mW and a pulse width from tens to hundreds of nanoseconds. A bitmap file, which was transformed automatically from an original picture, defined laser power of each pixel, writing path, and pixel stepping (50–200 nm, typically 150 nm).

Four optical images, one with two gray levels [Fig. 1(a)] and the others with continuous-tone gray levels [Figs. 1(b)–1(d)], were obtained using the LDW tech-

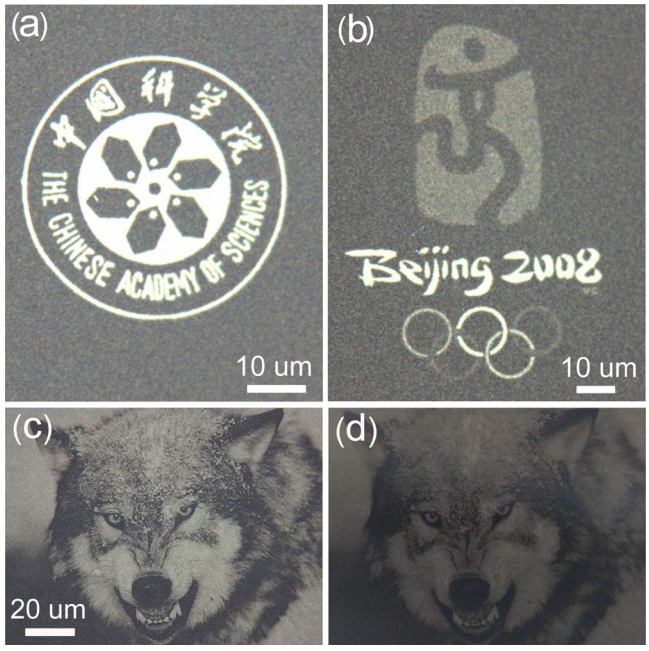

Fig. 1. (Color online) (a),(b) Optical images in Sn film created by the LDW technique; (c) and (d) are back-lit and front-lit images, where (d) is reverse processed.

0146-9592/09/182820-3/$15.00

nique. The gray levels were realized by adjusting writing power, where a high power yields a high transmittance and low reflectance. Each pixel of the image was assigned to a laser power to obtain a certain transmittance or reflectance; therefore both front-lit and back-lit images could be observed. The high-resolution optical images shown in Figs. 1(c) and 1(d) are a lifelike wolf in the snowfall with fine structures like furs and whiskers.

The optical images reflect the transmittance and reflectance versus the laser power, and the topography of the laser exposed areas can be observed by using atomic force microscopy (AFM, Veeco D-3100). Experimental data show that dependence of both the optical density and Δh on the laser power are almost linear (see Fig. 2); this presents great advantages in controllably fabricating fine optical images and complicated micro/nanoreliefs. As expected, AFM topographic images agree well with optical images, which means the laser exposed area not only has exact optical image replication in the film plane but also controllable height in the Z direction. Figure 3(a) shows an AFM topographic image of a wolf, which is very consistent with the corresponding optical image shown in Fig. 1(d). Its section analysis shows that heights (up to ~12 nm) can vary with different laser powers [see Fig. 3(b)], i.e., the Δh to the as-deposited metallic film thickness (t): $\Delta h/t$ can reach ~100%. Fine structures with a resolution of ~200 nm, smaller than the diffraction limit of 532 nm laser with an objective lens (NA=0.95), are observed [Fig. 3(c)]. This is very difficult to achieve by using the conventional photolithography technique. The results demonstrate that our LDW technique is competent to fabricate metallic nanoreliefs with superresolution fine structures and a continuously variable height. The high similarity of an AFM image and an optical image confirms that the writing power can continuously control not only transmittance and reflectance but also film thickness.

$$\mathrm{Sn} + (x/2)\mathrm{O}_2 \xrightarrow{\text{pulsed laser}} \mathrm{SnO}_x. \quad (1)$$

The LDW on Sn film is not a simple laser-induced thermal oxidation process as proposed in [14]. Oxidation of metallic films such as Ti and Sn can only lead to a limited increase in height [14,15]. The β-Sn is found to be transformed to amorphous (a-) SnO_x [defined as in Eq. (1)] instead of crystal oxides such as SnO or SnO_2 after laser exposure; however, this is

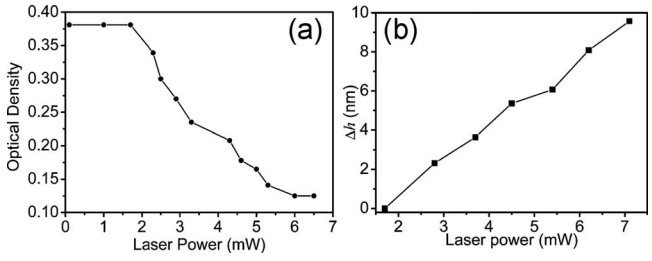

Fig. 2. Laser power versus (a) optical density at 532 nm and (b) Δh at a pulse width of 80 ns, both demonstrating nearly linear relationships.

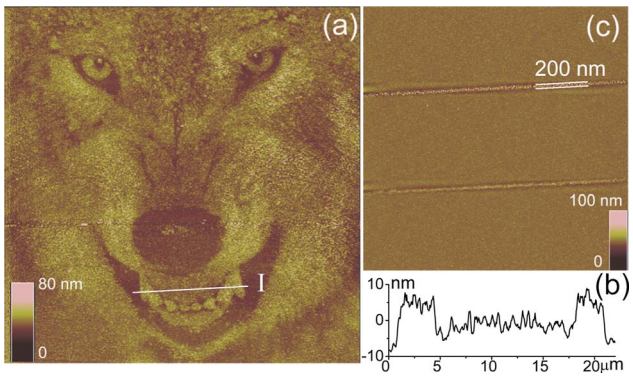

Fig. 3. (Color online) (a) AFM topographic image of the nanorelief (70 μm×70 μm) and (b) section analysis along the line "I." (c) AFM image (20 μm×20 μm) of raster-scanned lines with high resolution of ~200 nm.

not the main reason of the change in height. In fact, even if a 12-nm-thick Sn film is completely oxidized, it can have a thickness increase of only 4 nm, but actually we find Δh achieves 12 nm. A mechanism is proposed to solve the contradiction [see Fig. 4(a)]. The as-deposited Sn grains are coated by a thin a-SnO_x shell (~2 nm) and with a flat morphology [16,17]. Owing to the low melting point (232°C), the Sn grains tend to melt under laser exposure. At a fitting laser power, the Sn is melted to liquid Sn/SnO_x structures [18]; meanwhile, the balling effect occurs because the melt does not wet the underlying glass substrate; as a result, this spheroidized morphology is retained after cooling down. The balling effect can efficiently add the grain height. At a higher power, coarsening, which aggregates two or several adjacent

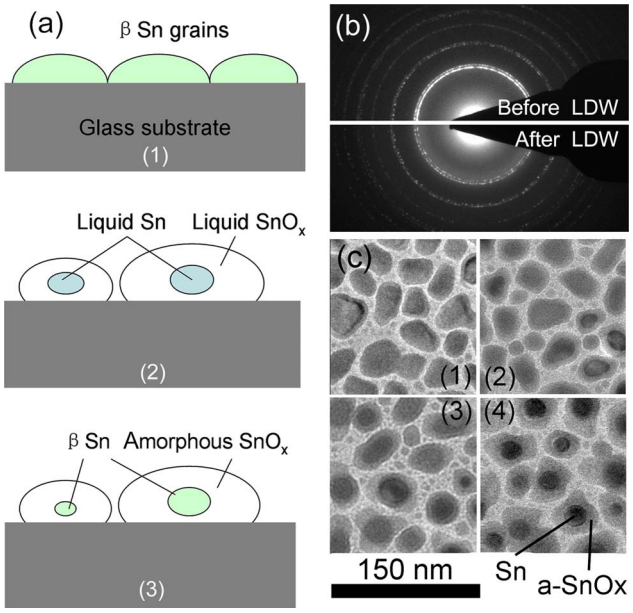

Fig. 4. (Color online) Mechanism of height change in the nanoreliefs. (a) Proposed model: (1) as-deposited Sn film with flat grains, (2) balling and coarsening of Sn grains induced by LDW, and (3) after cooling down. (b) SAED results verify the formation of Sn/a-SnO_x core/shell structure. (c) TEM image showing evolution of Sn/a-SnO_x core/shell structures: (1)–(4) are the film morphologies corresponding to different laser powers from low to high.

liquid Sn/SnO_x structures, will happen and lead to an additional height increase. The laser power can exactly control the temperature, thereby controlling the grain height. The β-Sn/a-SnO_x structure has already been directly confirmed by selected area electron diffraction (SAED) patterns and transmission electron microscopy (TEM) images [Figs. 4(b) and 4(c)]. The diffraction intensity of the bottom SAED pattern in Fig. 4(b) is weaker than that of the as-deposited film, revealing a decrease in the content of β-Sn after laser exposure. And a decrease in the diameter of the Sn core and an increase in thickness of the a-SnO_x shell with an increase of laser power has been observed, as shown in Fig. 4(c). To sum up, the height change of the Sn film is mainly contributed to from the balling of the flat-shaped grains; continuously variable transmittance and reflectance originate from the changes of components of Sn and a-SnO_x under various laser powers.

In summary, the nanoreliefs, based on the controllable change in thickness and continuous-tone optical properties of the Sn film, were successfully fabricated using the LDW technique. The optical density and height change are both nearly linear to the laser power. The laser-induced high temperature causes not only oxidation but also melting and resolidifying of the grains to add grain height. The controllable and relatively large Δh mainly comes from balling of the grains rather than the incorporation of oxygen atoms, consistent with the experimental results. The nanoreliefs are found to have high resolution ($\sim$200 nm) smaller than the diffraction limit of the 532 nm laser system and a height change up to 12 nm ($\Delta h_{max}/t = 100\%$). Gaussian distribution of laser energy might be a reason for the high resolution. The reduction of Sn (or increase of a-SnO_x) leads to the controllable transmittance and reflectance of the nanoreliefs. This work presents a way to fabricate complicated nanoreliefs by utilizing a laser-induced film thickening process, which differs from the current techniques such as photolithography, EBL, and FIB. The optical properties of the nanoreliefs reveal many potential applications in high-resolution optical images for micro/nano image storage, microartworks, and grayscale photomasks.

We thank Dr. Yongtao Fan and Prof. Wendong Xu for assistance with the LDW equipment. Funds of the 863 program (2006AA03Z353), the National Natural Science Foundation of China (NSFC) (90606025), the Knowledge Innovation Program of the Chinise Academy of Sciences (KIP CAS) (KJCX2-YW-M06), and the National Basic Research Program of China (NBRPC) (2010CB934102) are greatly acknowledged.

References

1. K. Reimer, H. J. Quenzer, M. Jürss, and B. Wagner, Proc. SPIE **3008**, 279 (1997).
2. T. Fujita, H. Nishihara, and J. Koyama, Opt. Lett. **7**, 578 (1982).
3. S. Y. Chou, P. R. Krauss, and P. Renstrom, Appl. Phys. Lett. **67**, 3114 (1995).
4. A. A. Tseng, Small **1**, 924 (2005).
5. K. Salaita, Y. H. Wang, and C. A. Mirkin, Nature Nanotech. **2**, 145 (2007).
6. K. Reimer, U. Hofmann, M. Juerss, W. Pilz, H. J. Quenzer, and B. Wagner, Proc. SPIE **3226**, 2 (1997).
7. J. Su, J. Du, J. Yao, F. Gao, Y. Guo, and Z. Cui, Proc. SPIE **3680**, 879 (1999).
8. W. Yu, X. Yuan, N. Ngo, W. Que, W. Cheong, and V. Koudriachov, Opt. Express **10**, 443 (2002).
9. E. Betzig and J. Trautman, Science **257**, 189 (1992).
10. J. B. Pendry, Phys. Rev. Lett. **85**, 3966 (2000).
11. S. Kawata, H. B. Sun, T. Tanaka, and K. Takada, Nature **412**, 697 (2001).
12. M. Deubel, G. von Freymann, M. Wegener, S. Pereira, K. Busch, and C. M. Soukoulis, Nature Mater. **3**, 444 (2004).
13. J. Wang, H. Xia, B. B. Xu, L. G. Niu, D. Wu, Q. D. Chen, and H. B. Sun, Opt. Lett. **34**, 581 (2009).
14. A. A. Gorbunov, H. Eichler, and W. Pompe, Appl. Phys. Lett. **69**, 19 (1996).
15. G. Carbajal-Franco, A. Tiburcio-Silver, U. J. M. Domınguez, and A. Sanchez-Juarez, Thin Solid Films **373**, 141 (2000).
16. E. P. Domashevskaya, O. A. Chuvenkova, V. M. Kashkarov, S. B. Kushev, S. V. Ryabtsev, S. Yu. Turishchev, and Yu. A. Yurakov, Surf. Interface Anal. **38**, 514 (2006).
17. J. G. Partridge, M. R. Field, J. L. Peng, A. Z. Sadek, K. Kalantar-zadeh, J. Du. Plessis, and D. G. McCulloch, Nanotechnology **19**, 125504 (2008).
18. A. Kolmakov, Y. Zhang, and M. Moskovits, Nano Lett. **3**, 1125 (2003).